

Global crop yield reductions due to surface ozone exposure: 2. Year 2030 potential crop production losses and economic damage under two scenarios of O₃ pollution

Shiri Avnery^a, Denise L. Mauzerall^{b,*}, Junfeng Liu^c, Larry W. Horowitz^c

^a Program in Science, Technology, and Environmental Policy, Woodrow Wilson School of Public and International Affairs, 414 Robertson Hall, Princeton University, Princeton, NJ 08544, USA

^b Woodrow Wilson School of Public and International Affairs, Department of Civil and Environmental Engineering, 445 Robertson Hall, Princeton University, Princeton, NJ 08544, USA

^c NOAA Geophysical Fluid Dynamics Laboratory, 201 Forrestal Road, Princeton University, Princeton, NJ 08540, USA

ARTICLE INFO

Article history:

Received 2 September 2010

Received in revised form

25 December 2010

Accepted 2 January 2011

Keywords:

Surface ozone

Ozone impacts

Agriculture

Crop loss

Integrated assessment

ABSTRACT

We examine the potential global risk of increasing surface ozone (O₃) exposure to three key staple crops (soybean, maize, and wheat) in the near future (year 2030) according to two trajectories of O₃ pollution: the Intergovernmental Panel on Climate Change Special Report on Emissions Scenarios (IPCC SRES) A2 and B1 storylines, which represent upper- and lower-boundary projections, respectively, of most O₃ precursor emissions in 2030. We use simulated hourly O₃ concentrations from the Model for Ozone and Related Chemical Tracers version 2.4 (MOZART-2), satellite-derived datasets of agricultural production, and field-based concentration:response relationships to calculate crop yield reductions resulting from O₃ exposure. We then calculate the associated crop production losses and their economic value. We compare our results to the estimated impact of O₃ on global agriculture in the year 2000, which we assessed in our companion paper [Avnery et al., 2011]. In the A2 scenario we find global year 2030 yield loss of wheat due to O₃ exposure ranges from 5.4 to 26% (a further reduction in yield of +1.5–10% from year 2000 values), 15–19% for soybean (reduction of +0.9–11%), and 4.4–8.7% for maize (reduction of +2.1–3.2%) depending on the metric used, with total global agricultural losses worth \$17–35 billion USD₂₀₀₀ annually (an increase of +\$6–17 billion in losses from 2000). Under the B1 scenario, we project less severe but still substantial reductions in yields in 2030: 4.0–17% for wheat (a further decrease in yield of +0.1–1.8% from 2000), 9.5–15% for soybean (decrease of +0.7–1.0%), and 2.5–6.0% for maize (decrease of +0.3–0.5%), with total losses worth \$12–21 billion annually (an increase of +\$1–3 billion in losses from 2000). Because our analysis uses crop data from the year 2000, which likely underestimates agricultural production in 2030 due to the need to feed a population increasing from approximately 6 to 8 billion people between 2000 and 2030, our calculations of crop production and economic losses are highly conservative. Our results suggest that O₃ pollution poses a growing threat to global food security even under an optimistic scenario of future ozone precursor emissions. Further efforts to reduce surface O₃ concentrations thus provide an excellent opportunity to increase global grain yields without the environmental degradation associated with additional fertilizer application or land cultivation.

© 2011 Elsevier Ltd. All rights reserved.

1. Introduction

Surface ozone (O₃) is the most damaging air pollutant to crops and ecosystems (Heagle, 1989). It is produced in the troposphere by catalytic reactions among nitrogen oxides (NO_x = NO + NO₂),

carbon monoxide (CO), methane (CH₄), and non-methane volatile organic compounds (NMVOCs) in the presence of sunlight. Ozone enters leaves through plant stomata during normal gas exchange. As a strong oxidant, ozone and its secondary byproducts damage vegetation by reducing photosynthesis and other important physiological functions, resulting in weaker, stunted plants, inferior crop quality, and decreased yields (Fiscus et al., 2005; Morgan et al., 2006; Booker et al., 2009; Fuhrer, 2009).

O₃ precursors are emitted by vehicles, power plants, biomass burning, and other sources of combustion. Over the past century, annual mean surface concentrations of ozone at mid- to high

* Corresponding author. Tel.: +1 609 258 2498; fax: +1 609 258 6082.

E-mail addresses: savnery@princeton.edu (S. Avnery), mauzeral@princeton.edu (D.L. Mauzerall), junfeng.liu@noaa.gov (J. Liu), larry.horowitz@noaa.gov (L.W. Horowitz).

latitudes have more than doubled (Hough and Derwent 1990; Marengo et al., 1994). Although O₃ mitigation efforts have reduced peak ozone levels in both rural and urban areas of North America, Europe, and Japan in recent years, background levels continue to increase (Oltmans et al., 2006). In addition, ozone concentrations are expected to rise in developing countries due to increased emissions of nitrogen oxides and other ozone precursors resulting from rapid industrialization (Nakićenović et al., 2000; Dentener et al., 2005; Riahi et al., 2007). Due to transport of O₃ pollution across national boundaries and continents (Fiore et al., 2009), rising O₃ precursor emissions in these nations are projected to increase hemispheric-scale background O₃ concentrations and hence may pose a threat to both local and global food security.

The demonstrated phytotoxicity of O₃ and its prevalence over important agricultural regions around the world demand an assessment of the magnitude and distribution of ozone risk to global food production under present-day and future O₃ concentrations. In the first of our two-part analysis (Avnery et al., 2011), we calculated global yield losses of three key staple crops (soybean, maize, and wheat) and their associated costs in the year 2000 using simulated O₃ concentrations by the Model for Ozone and Related Chemical Tracers version 2.4 (MOZART-2), observation-based crop production datasets, and concentration:response (CR) relationships derived from field studies. Our results indicated that year 2000 global yield reductions due to O₃ exposure ranged from 8.5–14% for soybean, 3.9–15% for wheat, and 2.2–5.5% for maize depending on the metric used, with global crop production losses (79–121 million metric tons (Mt)) worth \$11–18 billion annually (USD₂₀₀₀). These findings agree well with the only other estimate of global O₃-induced crop reductions and their economic value available in the literature (Van Dingenen et al., 2009), providing further evidence that the yields of major crops across the globe are already being significantly inhibited by exposure to surface ozone. Recent experimental- and observation-based studies support the results of model-derived estimates of regional and global crop losses (Feng and Kobayashi, 2009; Fishman et al., 2010).

Van Dingenen et al. (2009) additionally provide the first, and until now only, estimate of global crop yield losses due to ozone exposure in the near future (year 2030). Van Dingenen et al. (2009) calculate crop losses as projected under the optimistic “current legislation (CLE) scenario”, which assumes that presently approved air quality legislation will be fully implemented by 2030. They find that global crop yield reductions increase slightly from the year 2000 (+2–6% for wheat, +1–2% for rice, and +<1% for maize and soybean), with the most significant additional losses primarily occurring in developing nations. Unfortunately, the CLE scenario may be an overly optimistic projection of O₃ precursor emissions in many parts of the world, as enforcement often lags promulgation of air pollution regulations (Dentener et al., 2006). Van Dingenen et al. (2009) may have therefore significantly underestimated the future risk to agriculture from surface ozone.

Here we estimate potential future reductions in crop yields and their economic value due to O₃ exposure according to two different O₃ precursor emission scenarios: the Intergovernmental Panel on Climate Change (IPCC) Special Report on Emissions Scenarios (SRES) A2 and B1 storylines (Nakićenović et al., 2000), representing upper- and lower-boundary trajectories, respectively, of ozone precursor emissions. Through comparison with our year 2000 results, we identify agricultural winners and losers under each future scenario and nations where O₃ mitigation may be a particularly effective strategy to improve agricultural production without the environmental damage associated with conventional methods of increasing crop yields.

2. Methodology

2.1. Data sources

We use global crop production maps, simulated surface ozone concentrations from which we calculate O₃ exposure over crop growing seasons, and CR functions that relate a given level of ozone exposure to a predicted yield reduction to calculate global crop losses. Our first paper (Avnery et al., 2011) provides an in-depth description of our data sources and methods, which we briefly summarize and supplement here.

The global crop distribution datasets for the year 2000 (which we use for our 2030 analysis) were compiled by Monfreda et al. (2008) and Ramankutty et al. (2008). The authors used a data fusion technique, where two satellite-derived products (Boston University’s MODIS-based land cover product and the GLC2000 data set obtained from the VEGETATION sensor aboard SPOT4) were merged with national-, state-, and county-level crop area and yield statistics at 5 min by 5 min latitude–longitude resolution. We regrid their data to match the 2.8° × 2.8° resolution of MOZART-2.

We use the global chemical transport model (CTM) MOZART-2 (Horowitz et al., 2003, Horowitz, 2006) to simulate O₃ exposure according to precursor emissions specified by the IPCC SRES A2 and B1 scenarios (Nakićenović et al., 2000). MOZART-2 contains a detailed representation of tropospheric ozone–nitrogen oxide–hydrocarbon chemistry, simulating the concentrations and distributions of 63 gas-phase species and 11 aerosol and aerosol precursor species. The version of MOZART-2 we use is driven by meteorological inputs every three hours from the National Center for Atmospheric Research (NCAR) Community Climate Model (MACCM3) (Kiehl et al., 1998), and has a horizontal resolution of 2.8° latitude by 2.8° longitude, 34 hybrid sigma–pressure levels up to 4 hPa, and a 20-min time step for chemistry and transport. See Horowitz (2006) for a detailed description of the simulations used here.

Anthropogenic, biogenic, and biomass burning emission inventories for the year 1990 are described in detail in Horowitz et al. (2003) and Horowitz (2006). To obtain year 2030 anthropogenic emissions, anthropogenic emissions in 1990 were scaled by the ratio of 2030:1990 total emissions in four geopolitical regions (Table 1) as specified by the A2 and B1 emissions scenarios (available from <http://www.grida.no/climate/ipcc/emission/164.htm>). The A2 and B1 scenarios were chosen for analysis because they represent the upper- and lower-boundary projections, respectively, of most O₃ precursor emissions in the year 2030 (the exception being NMVOC emissions, which are highest under the A1B rather

Table 1

Scaling factors used with the 1990 base emissions in MOZART-2 to obtain year 2030 anthropogenic emissions under the A2 and B1 scenarios (Nakićenović et al., 2000).

	A2				B1			
	OECD ^a	REF ^b	Asia ^c	ALM ^d	OECD ^a	REF ^b	Asia ^c	ALM ^d
CH ₄	1.251	1.204	1.631	1.999	0.925	0.931	1.367	1.553
CO	0.973	0.680	1.855	1.522	0.649	0.295	1.192	0.471
NMVOC	1.084	1.590	1.534	1.676	0.685	0.695	1.230	1.060
NO _x	1.326	1.014	2.949	2.832	0.661	0.562	2.163	2.436
SO _x	0.410	0.705	3.198	3.006	0.238	0.406	1.650	3.195

^a ‘OECD’ refers to countries of the Organization for Economic Cooperation and Development as of 1990, including the US, Canada, western Europe, Japan and Australia.

^b ‘REF’ represents countries undergoing economic reform, including countries of eastern European and the newly independent states of the former Soviet Union.

^c ‘Asia’ refers to all developing countries in Asia, excluding the Middle East.

^d ‘ALM’ represents all developing countries in Africa, Latin America and the Middle East.

Table 2

Concentration:response equations used to calculate relative yield losses of soybean, maize, and wheat. RY = relative yield as compared to a theoretical yield without O₃-induced losses. Relative yield loss (RYL) is calculated as (1 – RY). See Section 2.2 for definitions of M7, M12 and AOT40. We calculate yield reductions for winter and spring wheat varieties separately and sum them together for our estimates of total O₃-induced wheat yield and crop production losses.

Crop	Exposure–relative yield relationship	Reference
Soybean	$RY = \exp[-(M12/107)^{1.58}]/\exp[-(20/107)^{1.58}]$	Adams et al. (1989)
	$RY = -0.0116 * AOT40 + 1.02$	Mills et al. (2007)
Maize	$RY = \exp[-(M12/124)^{2.83}]/\exp[-(20/124)^{2.83}]$	Lesser et al. (1990)
	$RY = -0.0036 * AOT40 + 1.02$	Mills et al. (2007)
Wheat	$RY = \exp[-(M7/137)^{2.34}]/\exp[-(25/137)^{2.34}]$	Lesser et al. (1990)
	$RY = \exp[-(M7/186)^{3.2}]/\exp[-(25/186)^{3.2}]$	Adams et al. (1989)
	$RY = -0.0161 * AOT40 + 0.99$	Mills et al. (2007)

than the A2 scenario). These scenarios are also opposite in terms of economic, environmental, and geopolitical driving forces, with the B1 scenario characterized by global cooperation and emphasis on environmental sustainability and the A2 scenario reflecting a more divisive world with greater importance placed on economic growth. Two-year simulations were performed with the first year used as spin-up and the second year results used for analysis.

In our first paper, we performed a detailed spatial evaluation of simulated year 2000 surface O₃ concentrations with observations according to the two metrics used to calculate O₃ exposure and yield losses (see Section 2.2 for metric definitions). We found that O₃ was fairly well-simulated over Europe and Asia, but that MOZART-2 systematically overestimated surface O₃ concentrations in the central and northeastern U.S. during the summer months, a bias commonly seen in many other global models (Reidmiller et al., 2009). Because the most significant overestimation of O₃ unfortunately occurs in areas of intensive crop production in the U.S., and because the U.S. is a major producer of all three crops analyzed in this study, we used O₃ concentration measurements over a span of five years (1998–2002) to bias-correct values of simulated O₃ exposure. We perform the same bias-correction here for our year 2030 analysis: we divide simulated O₃ exposure in the U.S. as calculated by the metrics defined in Section 2.2 over each crop growing season by the ratio of modeled:observed O₃ in the same grid cell where measurement data exist from 1998 to 2002 (where multiple observation sites exist in a single grid cell, we use the average of the measurements to correct simulated values). Where measurements do not exist, we use U.S. eastern and western regional averages of the modeled:observed ratio (dividing line of 90°W), as the model reproduces O₃ in the western U.S. much more accurately than in the East. Like our first paper, O₃ exposure,

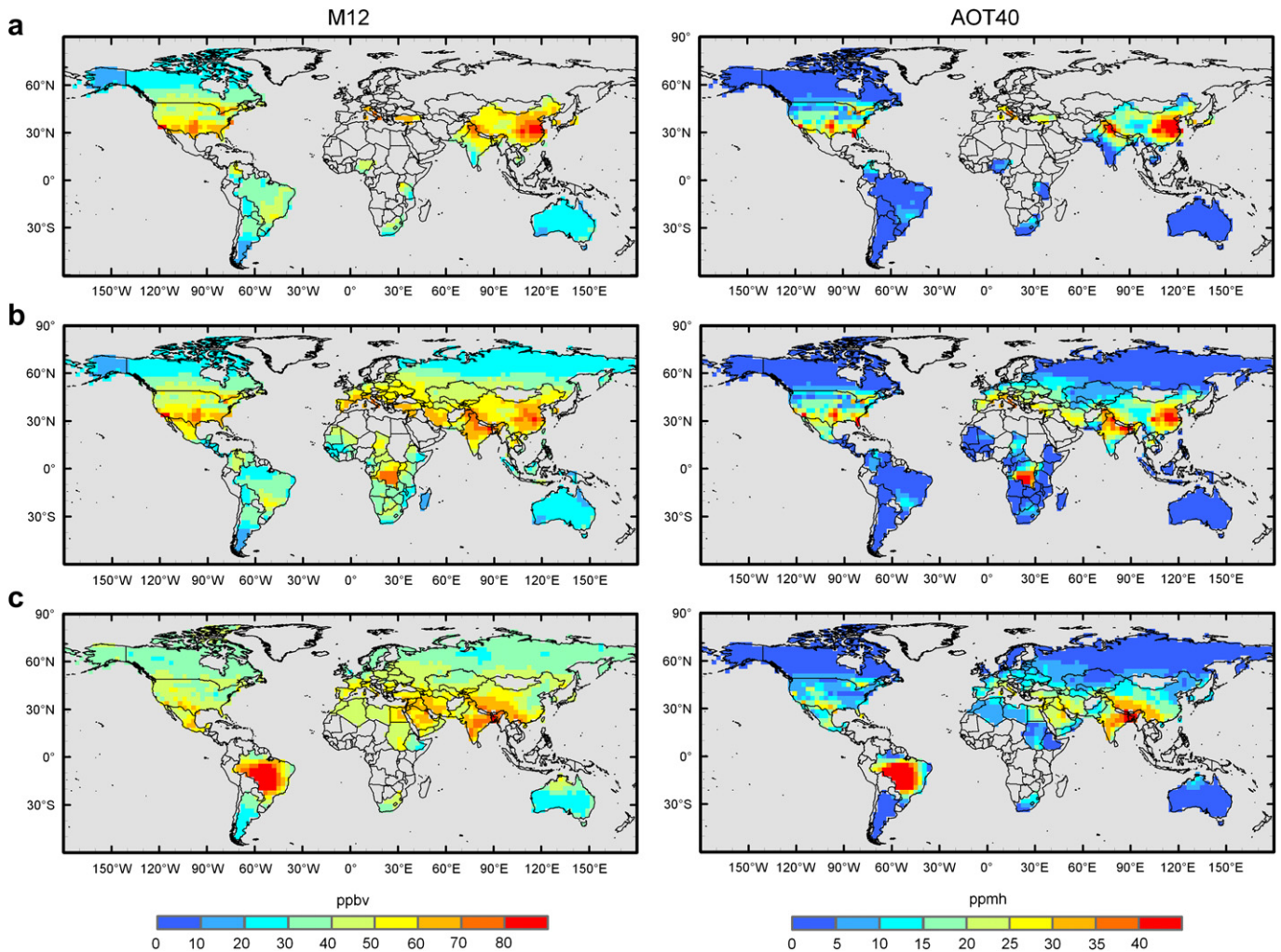


Fig. 1. Global distribution of O₃ exposure according to the M12 (left panels) and AOT40 (right panels) metrics under the 2030 A2 scenario during the respective growing seasons in each country (where crop calendar data are available) of (a) soybean, (b) maize, and (c) wheat. Minor producing nations not included in this analysis (where growing season data were unavailable) together account for <5% of global production of each crop. Values in the U.S. have been corrected using observation data as described in Section 2.1.

relative yield loss, crop production loss, and associated cost estimates presented in the following sections for the U.S. are based on these bias-corrected values of O₃ exposure. We recognize that applying the same bias-correction factors based on surface observations from the period 1998–2002 may not be accurate in the year 2030 due to the complicated non-linear chemistry associated with ozone formation. However, we believe this is the best approach given the presence of a systematic bias over the U.S. during the summer months and our inability to use alternative correction factors based on year 2030 surface observations.

2.2. Integrated assessment

Open-top chamber (OTC) field studies that took place primarily in the U.S. and Europe during the 1980s and 1990s established crop-specific concentration:response (CR) functions that predict the yield reduction of a crop at different levels of ozone exposure (Heagle, 1989; Heck, 1989; Krupa et al., 1998). O₃ exposure can be represented in numerous ways, with different statistical indices used to summarize the pattern of ambient O₃ during crop growing seasons. We implement two widely used metrics, M12 and AOT40, and their CR relationships (Table 2) to calculate crop yield losses globally:

$$M12 \text{ (ppbv)} = \frac{1}{n} \sum_{i=1}^n [Co_3]_i$$

$$AOT40 \text{ (ppmh)} = \sum_{i=1}^n ([Co_3]_i - 0.04) \text{ for } Co_3 \geq 0.04 \text{ ppmv}$$

where [Co₃]_i is the hourly mean O₃ concentration during daylight hours (8:00–19:59); and n is the number of hours in the 3-month growing season.

We substitute the highly correlated M7 metric (defined like M12 except with daylight hours from 9:00 to 15:59) when M12 parameter values have not been defined for certain crops. Estimates of soybean and maize (wheat) yield losses are generally larger (smaller) when the M12 rather than the AOT40 metric is used. However, the AOT40 index and CR functions predict greater losses for soybean at higher levels of O₃ exposure than the M12 metric. See Avnery et al. (2011) for further detail about these O₃ exposure metrics/CR functions and their associated uncertainties.

Using hourly surface O₃ simulated by MOZART-2, we calculate O₃ exposure according to the M12 (M7) and AOT40 metrics over the appropriate growing season for soybean, maize, and wheat in

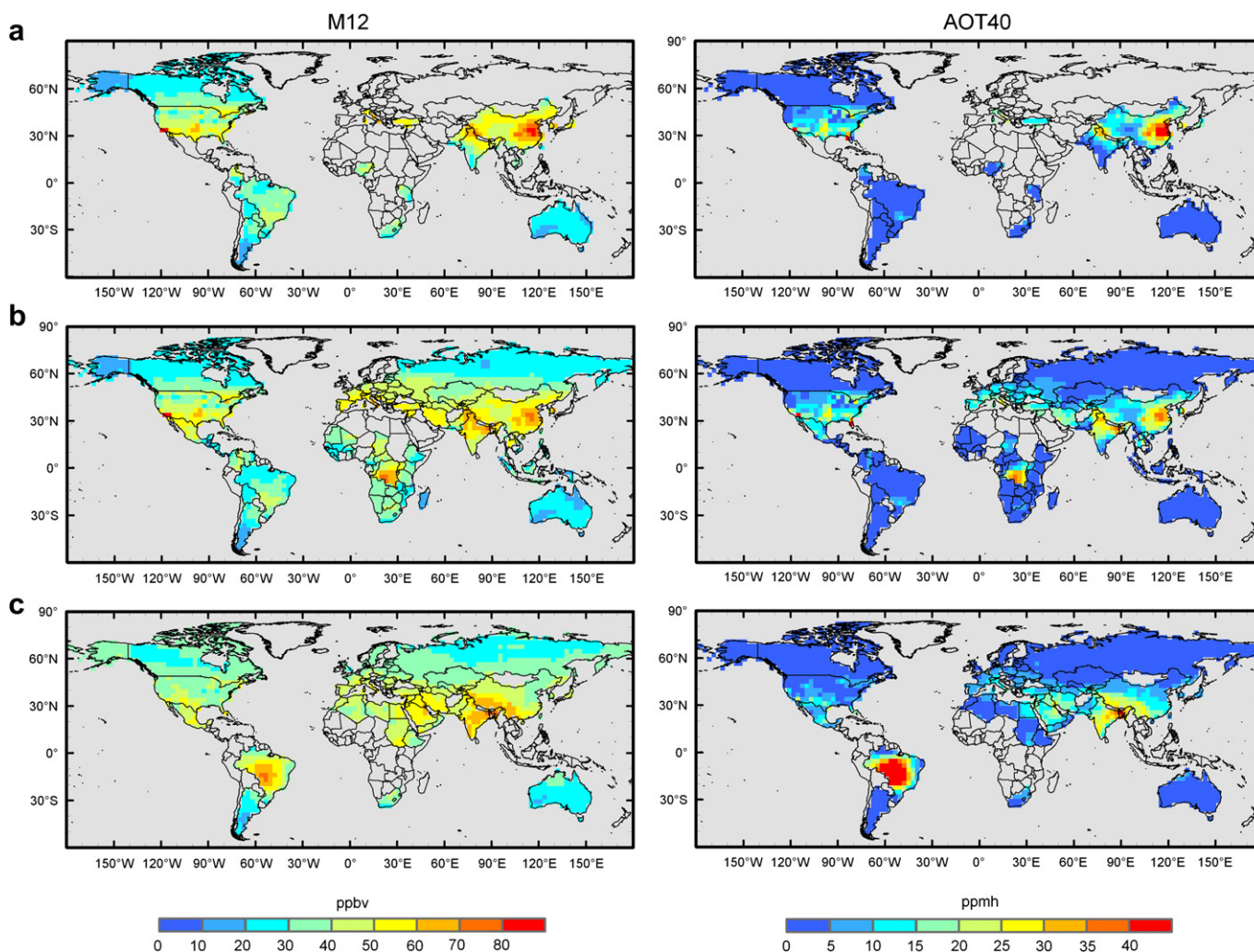


Fig. 2. Global distribution of O₃ exposure according to the M12 (left panels) and AOT40 (right panels) metrics under the 2030 B1 scenario during the respective growing seasons in each country (where crop calendar data are available) of (a) soybean, (b) maize, and (c) wheat. Minor producing nations not included in this analysis (where growing season data were unavailable) together account for <5% of global production of each crop. Values in the U.S. have been corrected using observation data as described in Section 2.1.

each $2.8^\circ \times 2.8^\circ$ grid cell. “Growing season” is here defined like in Van Dingenen et al. (2009) and Avnery et al. (2011) as the 3 months prior to the start of the harvest period according to crop calendar data from the United States Department of Agriculture (USDA); data are available for nations accounting for over 95% of global production of each crop examined here (USDA, 1994, 2008). We use our distributions of O_3 exposure and the CR functions defined in Table 2 to calculate relative yield loss (RYL) in every grid cell (RYL_i) for each crop. Relative yield loss is defined as the reduction in crop yield from the theoretical yield that would have resulted without O_3 -induced damages (see Table 2). Following Wang and Mauzerall (2004), we then calculate CPL in each grid cell (CPL_i) from RYL_i and the actual crop production in the year 2000 (CP_i) (Monfreda et al., 2008; Ramankutty et al., 2008) according to:

$$CPL_i = \frac{RYL_i}{1 - RYL_i} \times CP_i \quad (1)$$

National CPL is determined by summing crop production loss in all the grid cells within each country. We define national RYL as national CPL divided by the theoretical total crop production without O_3 injury (the sum of crop production loss and actual crop production in the year 2000). Because this calculation uses crop

data from the year 2000, which likely underestimates production in 2030 due to the projected growth in demand for food over the next few decades, our calculations of crop production losses are conservative. Finally, we implement a simple revenue approach to estimate economic loss by multiplying national CPL by producer prices for each crop in the year 2000 as given by the FAO Food Statistics Division (FAOSTAT, 2008, <http://faostat.fao.org/>). We use FAO producer prices as a proxy for domestic market prices due to insufficient information on actual crop prices. This approach has been found to produce estimates of economic loss that are within 20% of those derived using a general equilibrium model with factor feedbacks (Westenbarger and Frisvold, 1995).

3. Results

3.1. Distribution of crop exposure to O_3

Figs. 1 and 2 depict the global distribution of crop exposure to O_3 in 2030 according to the M12 and AOT40 metrics under the A2 and B1 scenarios, respectively. Figures illustrating the change in O_3 exposure from the year 2000 under each scenario are available in the Supplementary Material. O_3 is generally higher in the Northern Hemisphere, with exposure during the wheat growing season in

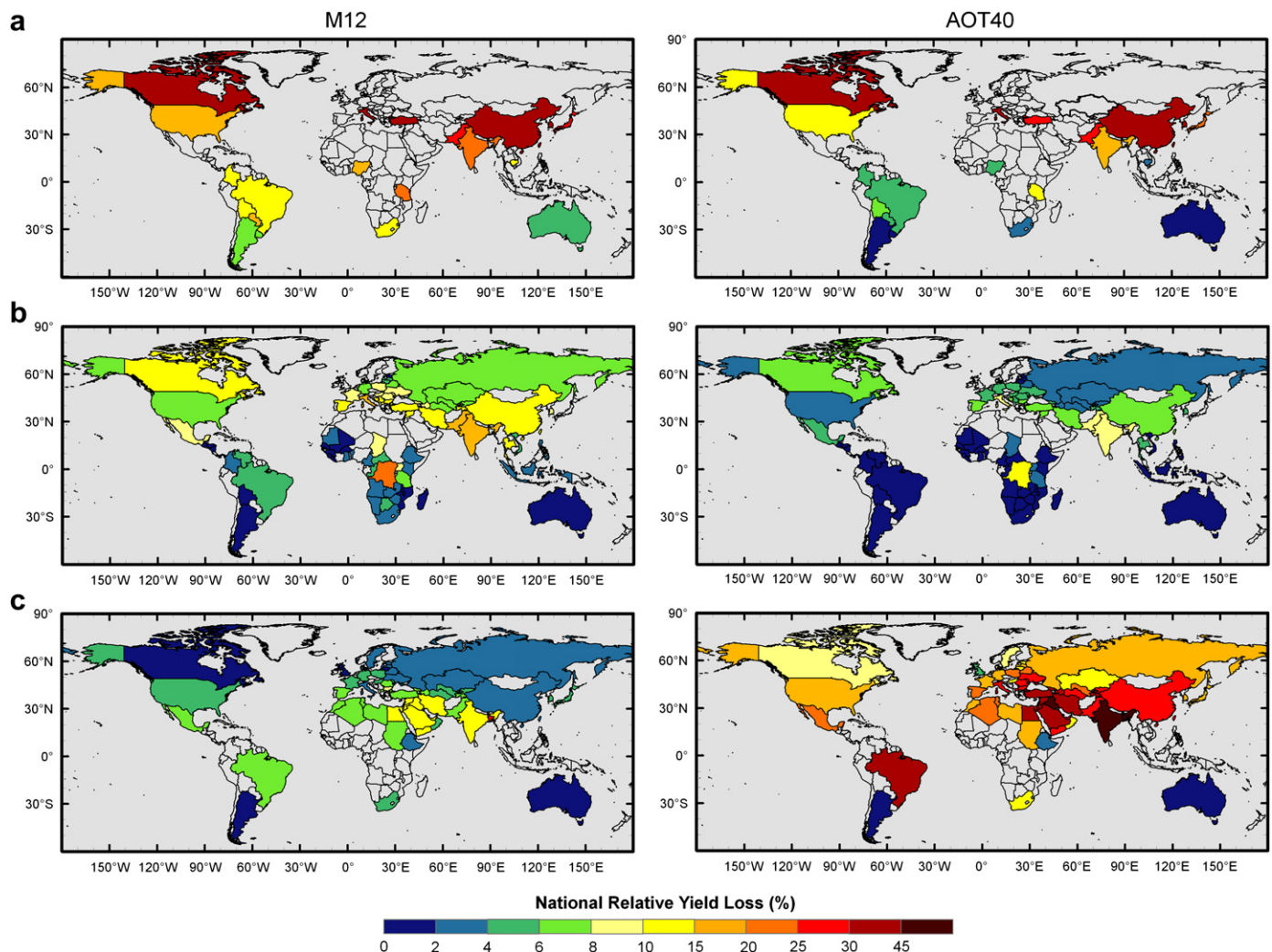


Fig. 3. National relative yield loss under the 2030 A2 scenario according to the M12 (left panels) and AOT40 (right panels) metrics for (a) soybean, (b) maize, and (c) wheat.

Table 3
Estimated year 2030 regional relative yield loss (%) due to O₃ exposure under the A2 scenario according to the M7, M12 and AOT40 metrics and the metric average.

	World	EU 25	FUSSR & E. Europe	N. Am	L. Am.	Africa & M.E.	E. Asia	S. Asia	ASEAN & Australia
<i>Wheat</i>									
AOT40	25.8	16.9	21.5	14.5	12.6	35.5	25.7	44.4	1.3
M7	5.4	4.5	4.0	3.1	3.0	9.4	3.8	11.2	0
Mean	15.6	10.7	12.7	8.8	7.8	22.4	14.7	27.8	0.6
<i>Maize</i>									
AOT40	4.4	5.9	5.1	3.4	1.2	1.6	7.9	8.9	2.3
M12	8.7	11.0	9.7	7.2	4.6	5.2	13.3	16.0	5.9
Mean	6.5	8.5	7.4	5.3	2.9	3.4	10.6	12.5	4.1
<i>Soybean</i>									
AOT40	19.0	32.8	-	15.7	3.2	7.8	40.6	15.6	1.4
M12	14.8	32.4	-	19.9	11.9	16.6	35.4	22.0	9.1
Mean	16.4	32.6	-	17.8	7.5	12.2	38.0	18.8	5.3

Brazil and during the maize growing season in the Democratic Republic of the Congo (DRC) also elevated in both futures (Figs. 1c and 2c). As noted in our companion paper, O₃ exposure during the soybean and maize growing seasons is particularly elevated in the Northern Hemisphere due to the coincidence of these crops'

growing seasons with peak summer O₃ concentrations, while the wheat and maize growing seasons in Brazil and the DRC, respectively, coincide with these nations' biomass burning seasons (Avnery et al., 2011).

In the A2 scenario, M12 ranges from 30 ppbv to over 80 ppbv for all three crops in the Northern Hemisphere while AOT40 ranges from zero to over 40 ppmh in northern India, eastern China, and parts of the U.S. (Fig. 1). Northern Hemisphere O₃ exposure is considerably lower in the B1 scenario. M12 ranges from 20 to 60 ppbv over most continental regions with higher exposures (>70 ppbv) limited to northern India, eastern China, and parts of the southern U.S. AOT40 is most reduced compared to the A2 scenario in the U.S., Europe, and the Middle East (Fig. 2); however, AOT40 in the B1 scenario still remains largely above the 3 ppmh "critical level" established in Europe for the protection of crops (Karenlampi and Skarby, 1996), particularly during the soybean and maize growing seasons. M12 in the Southern Hemisphere ranges from 10 to 40 ppbv in both scenarios with the exception of Brazil during the wheat growing season and the DRC during the maize growing season, where M12 O₃ reaches 80 ppbv. AOT40 in the Southern Hemisphere is largely below 5 ppmh for both scenarios with the exception of the two nations listed above, as well as South Africa and parts of northern Australia (Figs. 1 and 2).

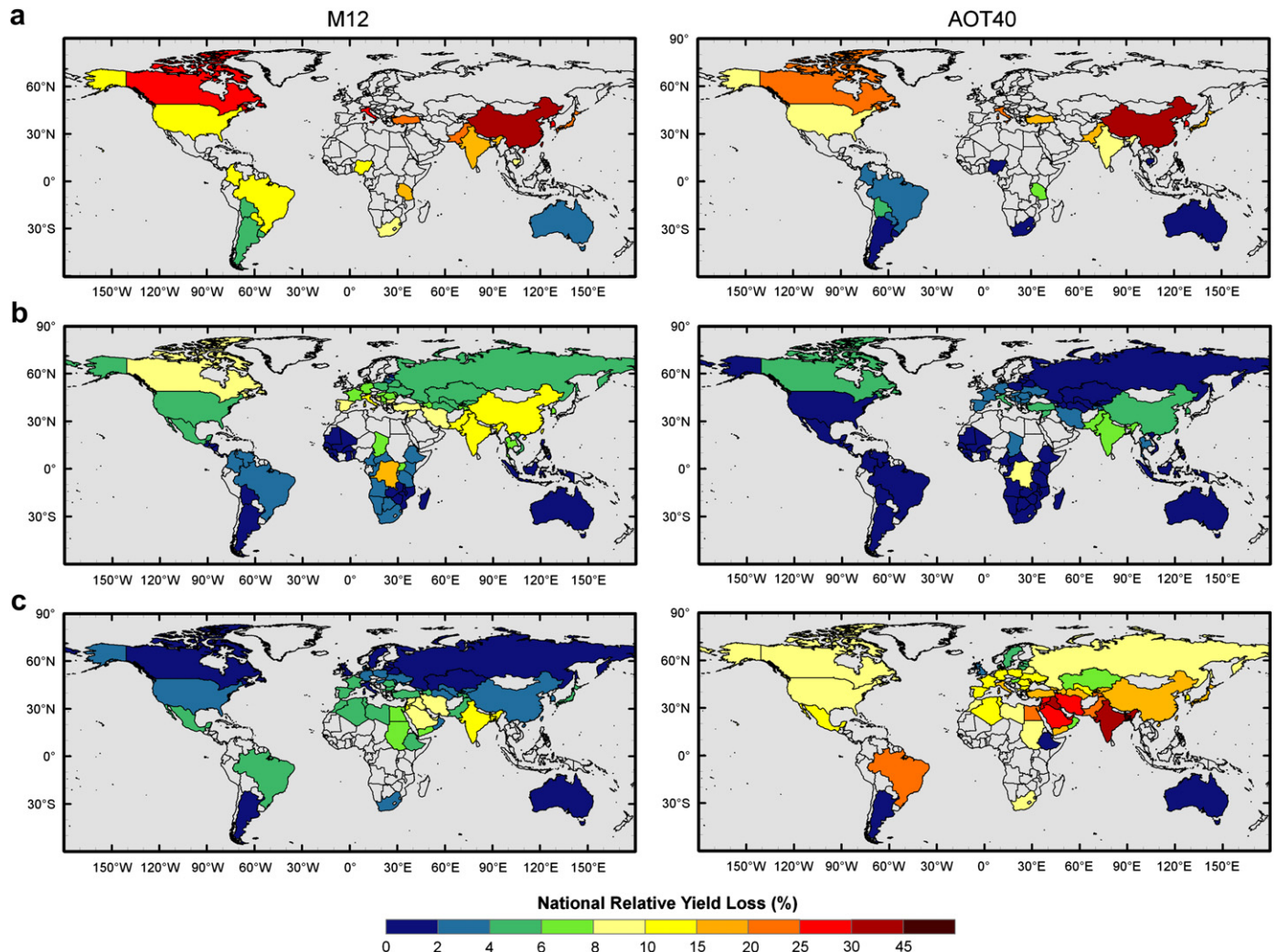


Fig. 4. National relative yield loss under the 2030 B1 scenario according to the M12 (left panels) and AOT40 (right panels) metrics for (a) soybean, (b) maize, and (c) wheat.

Table 4
Estimated year 2030 regional relative yield loss (%) due to O₃ exposure under the B1 scenario according to the M7, M12 and AOT40 metrics and the metric average.

	World	EU 25	FUSSR & E. Europe	N. Am	L. Am.	Africa & M.E.	E. Asia	S. Asia	ASEAN & Australia
<i>Wheat</i>									
AOT40	17.2	10.4	11.4	8.2	8.1	21.4	19.7	33.8	1.0
M7	4.0	3.4	2.4	2.0	2.6	6.4	3.1	9.2	0
Mean	10.6	6.9	6.9	5.1	5.4	13.9	11.4	21.5	0.5
<i>Maize</i>									
AOT40	2.5	2.9	2.2	1.6	0.4	0.8	5.8	6.3	1.2
M12	6.0	7.2	6.4	4.4	3.3	3.6	10.3	12.0	4.0
Mean	4.3	5.0	4.3	3.0	1.9	2.2	8.0	9.1	2.6
<i>Soybean</i>									
AOT40	9.5	20.4	-	9.8	1.7	3.0	31.5	8.6	0.1
M12	14.6	25.3	-	14.6	9.4	13.3	30.5	17.6	5.7
Mean	12.1	22.9	-	12.2	5.5	8.2	31.0	13.1	2.9

3.2. Relative yield loss

3.2.1. RYL year 2030 – A2

Fig. 3 depicts the global distribution of national RYL due to O₃ exposure for each crop and metric in 2030 under the A2 scenario, while Table 3 presents regionally aggregated and global RYL results (see Avnery et al. (2011) for regional definitions). O₃-induced RYL of wheat is greatest in Bangladesh (26–80%), Iraq (14–47%), India (12–48%), Jordan (14–44%), and Saudi Arabia (13–43%), depending on the metric used. The extremely high projected RYL in Bangladesh according to the AOT40 metric is due to a predicted O₃ exposure of over 40 ppmh during the growing season. It is possible that this value is overestimated by MOZART-2; however, we are unable to evaluate our simulated concentrations in this region because no O₃ observations are available. For context, Beig et al. (2008) calculated AOT40 from observations in

Pune, India between 2003 and 2006 and report values near 23 ppmh during the wheat growing season in India (January–March). At this location MOZART-2 predicts a value of 20 ppmh in 2000 over these months. Pune is located in western India, however, where O₃ concentrations tend to be lower than eastern India and Bangladesh during winter (the Bangladeshi wheat growing season).

Although O₃ is elevated during the wheat growing season over much of central Brazil (Fig. 1c), most of this nation’s wheat is grown in the south where O₃ exposure is significantly lower. Like the year 2000 scenario, there is a large range of RYL for wheat because this crop appears to be resistant to O₃ exposure according to the M12 metric, but extremely sensitive to ozone according to the AOT40 index. This discrepancy may be a consequence of the possibility that wheat is more sensitive to frequent exposure to high O₃ concentrations (better captured by AOT40) than to long-term exposure to moderate ozone concentrations (better captured by the mean metric) (Wang and Mauzerall, 2004). Soybean RYL under the A2 scenario is estimated to be greatest in China (35–40%), Canada (32–34%), Italy (32–33%), South Korea (31%), and Turkey (27–30%). Yield losses of maize are smaller but still substantial, with the highest losses occurring in the DRC (12–21%), Italy (10–16%), Pakistan (9.1–16%), India (8.9–16%), and Turkey (7.6–14%). Overall, global RYL totals 5.4–26% for wheat, 15–19% for soybean, and 4.4–8.7% for maize (Table 3).

Table S1 lists the estimated increases in regionally and globally aggregated RYL under the A2 scenario relative to year 2000 (RYL₂₀₃₀ – RYL₂₀₀₀). On a global scale, O₃-induced RYL is estimated to increase by +1.5–10% for wheat, +0.9–10% for soybean, and +2.1–3.2% for maize in 2030. South Asia is projected to suffer the greatest additional wheat RYL (+10% according to the average of metric estimates) followed by Africa and the Middle East (+9.4%), Eastern Europe (+5.8%) and East Asia (+5.0%). Increased soybean yield losses are estimated to be greatest in East Asia (+15%), South

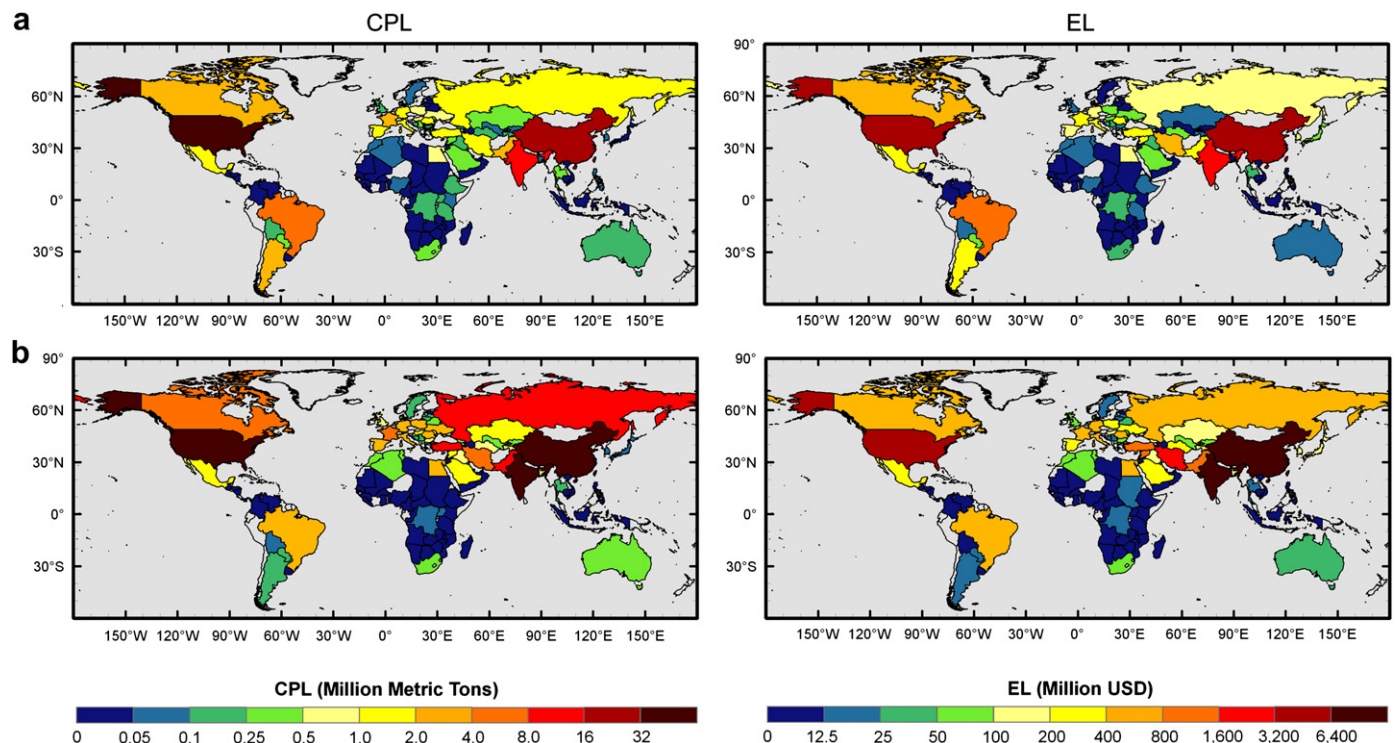


Fig. 5. Total crop production loss (CPL, left panels) and economic loss (EL, right panels) under the 2030 A2 scenario for all three crops derived from (a) M12 and (b) AOT40 estimates of O₃ exposure.

Asia (+11%), the EU25 (+7.0%), and Africa and the Middle East (+6.2%). Additional RYL of maize is projected to occur primarily in South and East Asia (+6.8 and +4.7%, respectively), but with increased losses of $\sim +3\%$ also estimated for the EU25 and Eastern Europe.

3.2.2. RYL year 2030 – B1

Fig. 4 depicts the global distribution of national RYL for each crop and metric in 2030 under the B1 scenario, while Table 4 presents regionally aggregated and global RYL results. O_3 -induced RYL of wheat is greatest in Bangladesh (15–65%), India (10–37%), Iraq (10–33%), Jordan (10–30%), and Saudi Arabia (10–29%). RYL in Bangladesh is again calculated to be extremely high, as O_3 exposure is projected to be only slightly lower than under the A2 scenario (35–40 ppmh). Soybean RYL in the B1 scenario is projected to be greatest in China (31–32%), South Korea (26–28%), Canada (24–26%), Italy (20–25%), and Pakistan (18–24%). The highest estimated yield loss of maize is expected to occur in the DRC (8.7–16%), India (6.3–12%), Pakistan (6.3–12%), China (5.8–10%), and Italy (5.1–10%). On a global scale, RYL totals 4.0–17% for wheat, 10–15% for soybean, and 2.5–6.0% for maize under the B1 scenario (Table 4).

Table S2 lists the projected change in regionally and globally aggregated RYL estimates for 2030 under the B1 scenario relative to 2000. Globally, O_3 -induced RYL in this more optimistic future is estimated to worsen only slightly from 2000 levels with yields reduced an additional +0.1–1.8% for wheat, +0.7–1.0% for soybean,

and +0.3–0.5% for maize. Regional discrepancies are apparent, however, due to differences in projected O_3 precursor emissions among industrialized versus emerging economies. Year 2030 wheat yields decrease in South Asia by +4.1% on average, with less severe additional losses ($\sim +1$ –2%) predicted for other developing regions (Latin America, East Asia, and Africa and the Middle East). North America and the EU25 are projected to experience yield gains of wheat as compared to the year 2000 (change in RYL of -1.7% and -0.8% , respectively). Additional yield reductions of soybean are projected to occur primarily in East and South Asia (+8.2 and +4.9%, respectively), with increased losses of $\sim +2\%$ also estimated for Latin America and Africa and the Middle East. Soybean yield gains (change in RYL of -2 to -3%) are projected for the EU25 and North America. South and East Asia are further expected to suffer additional maize losses under the B1 scenario (+3.5% and +2.2%, respectively); maize RYL in other regions remains largely unchanged from the year 2000.

3.3. Crop production loss (CPL) and associated economic losses (EL)

3.3.1. CPL and EL year 2030 – A2

The combined year 2030 global crop production and economic losses due to O_3 exposure under the A2 scenario are illustrated in Fig. 5. Figs. 6 and 7 depict the change in CPL and EL, respectively, for the ten countries with the greatest absolute difference (2030 A2 – 2000) for each crop individually and combined. The change in regionally aggregated and global CPL for each crop, as well as

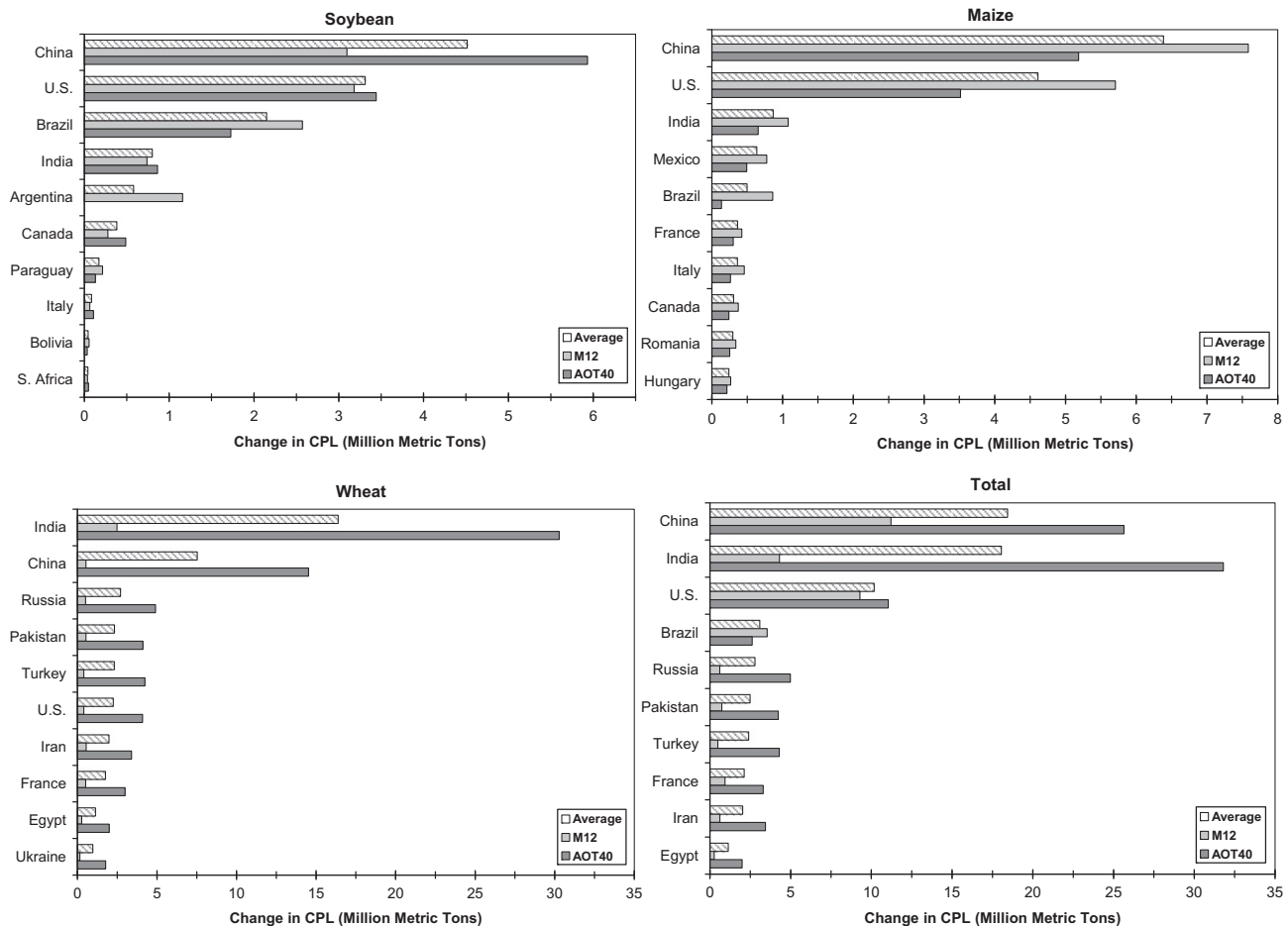


Fig. 6. Change in crop production loss (CPL, million metric tons) for the ten countries with highest absolute difference in estimated mean CPL between 2000 and 2030 under the A2 scenario using the M12 and AOT40 metrics for a) soybean, b) maize, c) wheat, and d) total CPL.

absolute year 2030 CPL, is presented in Tables S3 and S4 of the Supplementary Material. We calculate global CPL in the A2 scenario to be 29–178 Mt of wheat (a decrease in production of +9–85 Mt from the year 2000), 25–53 Mt of maize (decrease of +13–20 Mt), and 28–37 Mt of soybean (decrease of +11–13 Mt). South Asia is estimated to suffer the highest additional loss of wheat (19 Mt, average of metric estimates), while East Asia is projected to experience the greatest additional CPL of maize (6.4 Mt) and soybean (4.5 Mt) (Table S3). Total wheat CPL is highest in India (8.5–56 Mt) and China (3.7–33 Mt), followed by the U.S. (2.5–12 Mt). The U.S. is expected to suffer the greatest overall soybean loss (13–18 Mt), followed by China (7.7–10 Mt) and Brazil (1.8–5.7 Mt). CPL of maize is projected to be highest in China (9.7–17 Mt) and the U.S. (8.1–18 Mt), followed by India (1.0–1.9 Mt). On average, global CPL for all three crops totals 175 Mt (Table S4); this value represents a 75% increase over our average year 2000 CPL estimate (Avnery et al., 2011). We estimate that global EL due to O₃-induced yield losses totals \$17–35 billion USD₂₀₀₀ annually under the A2 scenario, an increase of +\$6–17 billion in damages from the year 2000. Most of the economic losses, both in absolute terms and in terms of the greatest change from year 2000 values, occur in China (\$5.6 billion, an increased loss of +\$2.6 billion from 2000), India (\$5.2 billion, +\$2.7 billion), and the U.S. (\$4.2 billion, +\$1.1 billion) (Fig. 7). Other countries with notable losses include Iran (over \$1 billion) and Brazil, Turkey, Pakistan, and Syria also each estimated to lose crop value worth \$500 million annually.

3.3.2. CPL and EL year 2030 – B1

Combined year 2030 global crop production and economic losses in the B1 scenario are illustrated in Fig. 8, while Figs. 9 and 10 depict the change in CPL and EL, respectively, for the ten countries with the greatest absolute difference (2030 B1 – 2000) for each crop individually and combined. The change in regionally aggregated and global CPL for each crop, as well as absolute year 2030 CPL under the B1 scenario, is presented in Tables S5 and S6 of the Supplementary Material. We estimate year 2030 global CPL to be 21–106 Mt of wheat (a decrease in production of +0.8–13 Mt from the year 2000), 14–35 Mt of maize (decrease of +1.7–2.9 Mt), and 17–27 Mt of soybean (decrease of +1.5–1.9 Mt). We calculate that South Asia will experience the greatest additional wheat CPL in this scenario, but the magnitude is greatly reduced compared to the A2 future (mean estimate of +6.4 Mt as opposed to +19 Mt). The same is true for additional maize and soybean CPL in East Asia, where increases over year 2000 estimates are projected to be +2–3 Mt for each crop (metric averages) (Table S5). Notably, production gains of 5–6 Mt of soybean, maize, and wheat are projected in North America due to reductions in O₃ precursors anticipated under the B1 scenario (Table 1). Thus, relative to 2000, developed countries experience modest yield and crop production gains in the optimistic B1 future, while developing countries suffer higher crop losses due to increased O₃ pollution (although these losses are not as severe as predicted for the A2 scenario).

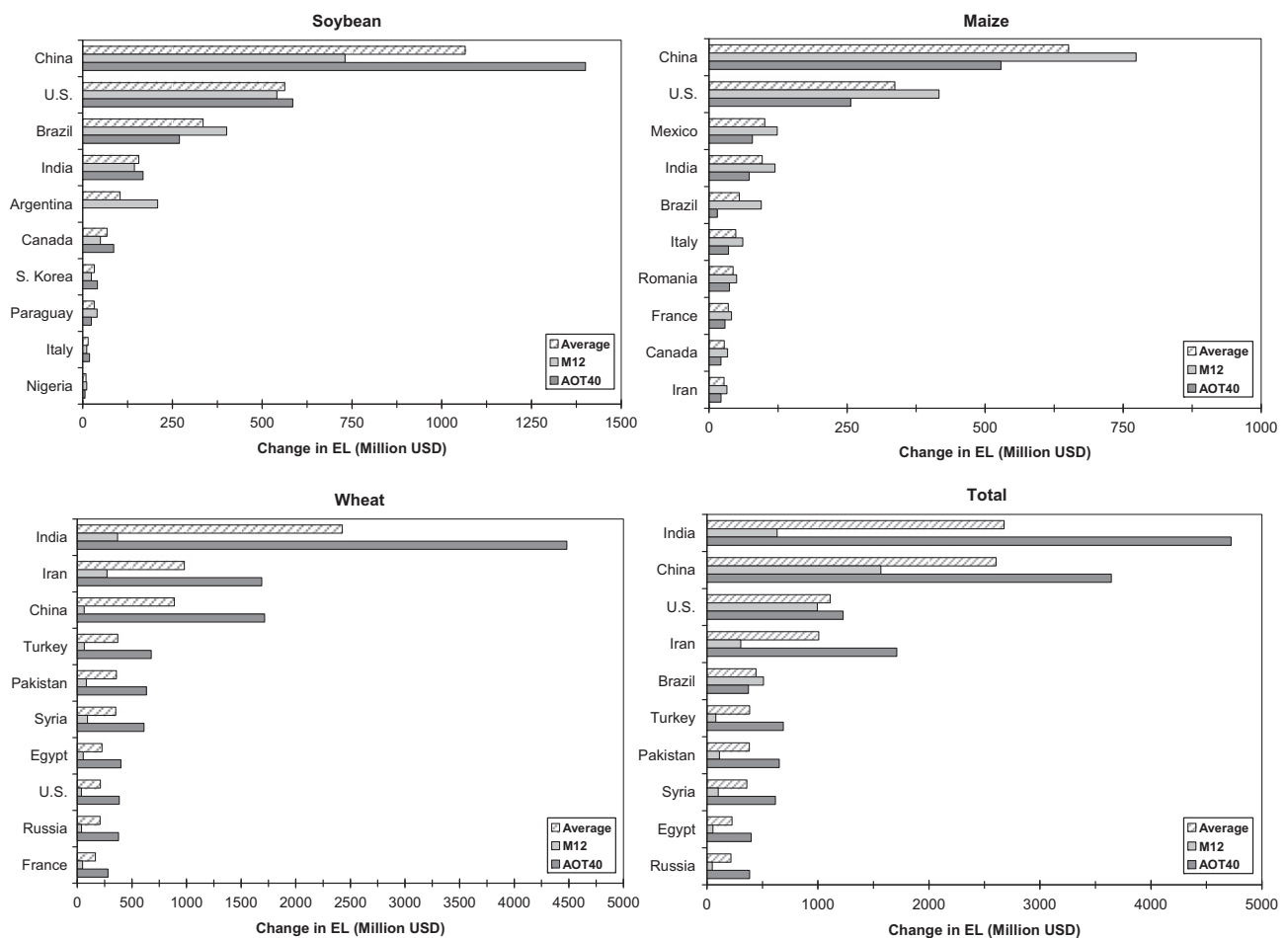


Fig. 7. Change in economic loss (EL, million USD₂₀₀₀) for the ten countries with highest absolute difference in estimated mean EL between 2000 and 2030 under the A2 scenario using the M12 and AOT40 metrics for a) soybean, b) maize, c) wheat, and d) total EL.

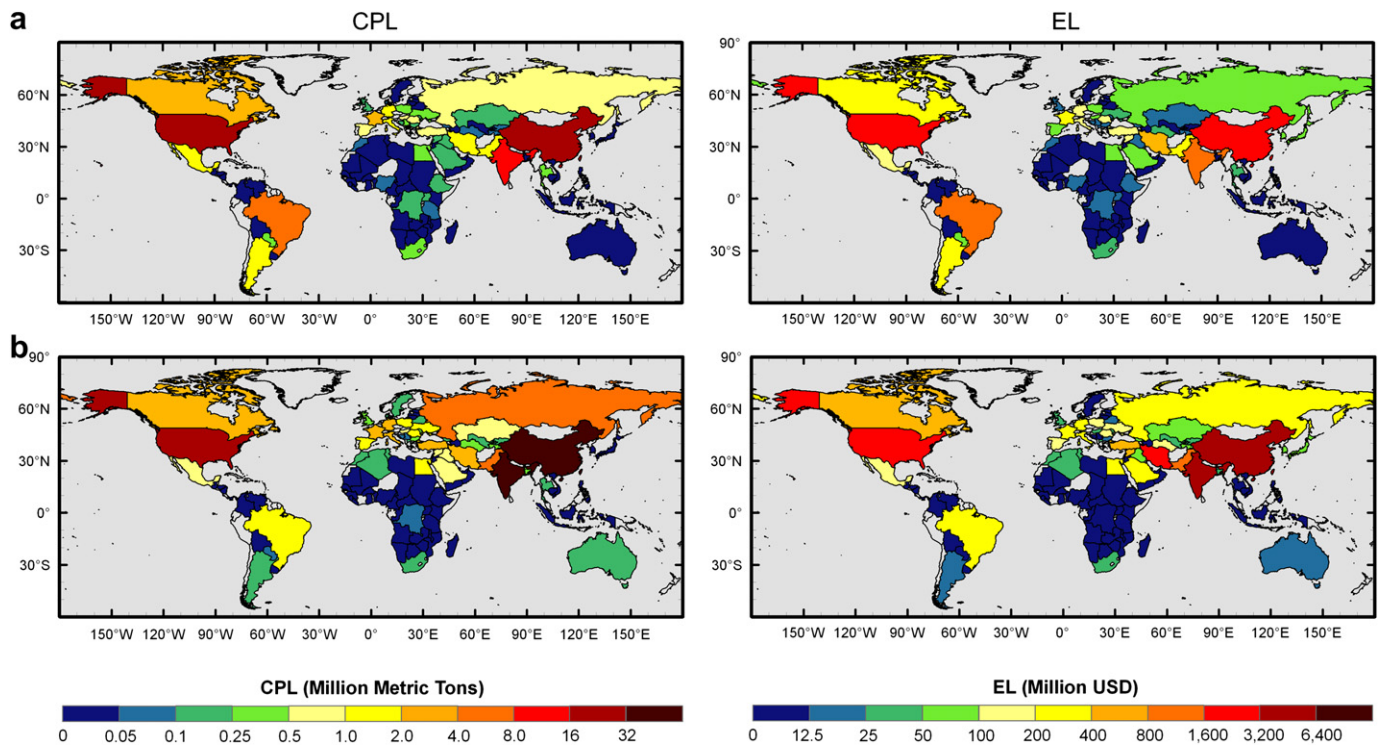


Fig. 8. Total crop production loss (CPL, left panels) and economic loss (EL, right panels) under the 2030 B1 scenario for all three crops derived from (a) M12 and (b) AOT40 estimates of O_3 exposure.

As in the A2 future, wheat CPL is greatest in India (6.9–35 Mt) and China (3.0–24 Mt), followed by the U.S. (1.6–5.3 Mt). Overall soybean CPL is expected to be highest in the U.S. (7.3–12 Mt), followed by China (6.2–6.5 Mt) and Brazil (0.9–4.6 Mt). Finally, maize CPL is projected to be highest in China (6.9–13 Mt) and the U.S. (3.7–11 Mt), followed by India (0.7–1.4 Mt). Global CPL for all three crops totals 84–137 Mt (Table S6), approximately 10% greater than our mean year 2000 estimate (Avnery et al., 2011). We estimate global EL in the B1 scenario to total \$12–21 billion USD₂₀₀₀ annually, an increase in O_3 -induced damages of +\$1–3 billion from the year 2000. The majority of the economic losses are expected to occur in China (\$4.1 billion, an increase in losses of +\$1.1 billion from the year 2000), India (\$3.4 billion, +\$0.9 billion), and the U.S. (\$2.5 billion, –\$0.6 billion). The U.S., Italy, Japan, and Canada experience monetary gains as compared to the year 2000 due to crop production improvements resulting from decreases in surface O_3 , although gains in the U.S. are an order of magnitude greater than those of other industrialized nations (Fig. 10). It is important to highlight the fact that despite crop recovery in the U.S. under the B1 scenario, this nation is still among the top three in terms of CPL for each major crop, and is further the third greatest economic loser due to O_3 -induced crop losses.

4. Discussion

4.1. Uncertainties

In our companion paper (Avnery et al., 2011), we provided a detailed review of the most important sources of uncertainty associated with the integrated assessment approach we use for our analysis (for brevity, only new sources of uncertainty are highlighted here). A major source of uncertainty is the ability of a global CTM to accurately simulate hourly surface O_3 concentrations to calculate crop losses. Predicting future O_3 concentrations is more difficult

because of: 1) uncertainty of future emissions of O_3 precursors; 2) inability to use surface observations to evaluate and bias-correct model simulations; and 3) potential feedbacks between climate change and O_3 concentrations over the next few decades that are not accounted for by CTMs. We attempt to address the first of these uncertainties by constraining potential future yield losses with optimistic and pessimistic projections of O_3 precursor emissions from the widely used IPCC SRES scenarios (Nakićenović et al., 2000). Although we cannot perform a model evaluation with surface observations from the year 2030, we use as a proxy bias-correction factors derived from observations in the years 1998–2002 and the year 2000 simulation (Avnery et al., 2011), as we expect similar regional biases in our future simulations. Finally, while future predictions of O_3 will be complicated by the potential feedbacks between climate change and ozone, as changes in temperature, precipitation, atmospheric circulation, and other local conditions can affect ozone concentrations that can in turn impact local and regional climate (e.g. Brasseur et al., 2006; Levy et al., 2008; Wu et al., 2008, Jacob and Winner, 2009; Ming and Ramaswamy, 2009), we expect any changes in O_3 concentrations and distributions due to such feedbacks to be of second order compared to those driven by anthropogenic emissions of ozone precursors.

Climate change may also influence our estimates of future crop yield reductions through altering stomatal conductance: increased temperatures and atmospheric CO_2 concentrations and decreased humidity and soil water content may reduce stomatal openings and therefore the amount of O_3 that enters plant leaves (Mauzerall and Wang, 2001; Fuhrer, 2009). In non-irrigated agricultural areas prone to water stress, this effect may be especially significant and may mitigate projected ozone damage. Additionally, climate change may directly impact crop yields through changes in temperature, precipitation patterns, and CO_2 fertilization—however, little is known about the combined effect of climate change and O_3 pollution on agriculture. To investigate this issue, Reilly et al.

(2007) use the MIT Integrated Global Systems Model, which includes an updated version of the biogeochemical Terrestrial Ecosystem Model (TEM) that simulates the impact of both climate change and surface ozone on plant productivity. The authors find that while the effects of climate change are generally positive in mid- to high latitudes, ozone pollution may more than offset potential climate benefits. For example, yield gains of 50–100% are predicted for some regions in the year 2100 when only climate impacts are considered, but inclusion of the model's O₃ damage function produces drastic yield reductions: combined climate and O₃ effects reduce yields by 43% in the U.S., 56% in Europe, 45% in India, 64% in China, and 80% in Japan. These results underscore the imperative for field studies that examine the combined impact on agricultural production of climate change and surface O₃ in order to evaluate model-based studies and to identify crop cultivars that are relatively robust to both O₃ and climate change.

Finally, climate change can indirectly affect our estimates of O₃-induced crop yield reductions through its impact on crop growing seasons and crop distributions, which we assume to be the same in our year 2030 analysis as the year 2000. We also do not account for potential adaptation measures farmers may embrace to maximize crop yields in the face of a changing climate or O₃ pollution, such as altering planting/harvesting dates, application of additional fertilizer/water through irrigation, or the development of new cultivars and irrigation infrastructure. Future work should account for potential adaptation through the use of a state-of-the-art agro-economic model, and should also consider feedbacks between crop

yields, production areas, and commodity prices to generate a more accurate estimate of the economic cost of agricultural losses.

We compare our results with those of similar studies which calculate future RYL, CPL, and EL in the [Supplementary Material](#). Despite differences in datasets, methodologies, model chemistry, and model simulations used among the studies, our results agree well with existing estimates of future O₃-induced crop losses and add to the literature by providing a broader range of possible future emissions of ozone precursors and their implications for global agricultural yields.

4.2. Policy implications

Between 2000 and 2030 global population is projected to increase from approximately 6 to over 8 billion persons ([US Census Bureau, 2010](#)), with global agricultural demand expected to double due to population growth, rising demand for biofuels, and increased meat consumption particularly in developing nations ([Tilman et al., 2002](#); [Edgerton, 2009](#)). To meet this future demand, we will need to either bring new terrain under cultivation, or increase productivity (i.e. yields) on existing agricultural land. The latter option is preferable in order to preserve remaining natural ecosystems and prevent the associated loss of biodiversity and increased greenhouse gas emissions. However, improving yields on land currently cultivated through traditional strategies—i.e., increasing agricultural inputs (water, fertilizer, pesticides)—also has detrimental environmental consequences ([Tilman et al., 2001](#)). Furthermore, research suggests that in the absence of

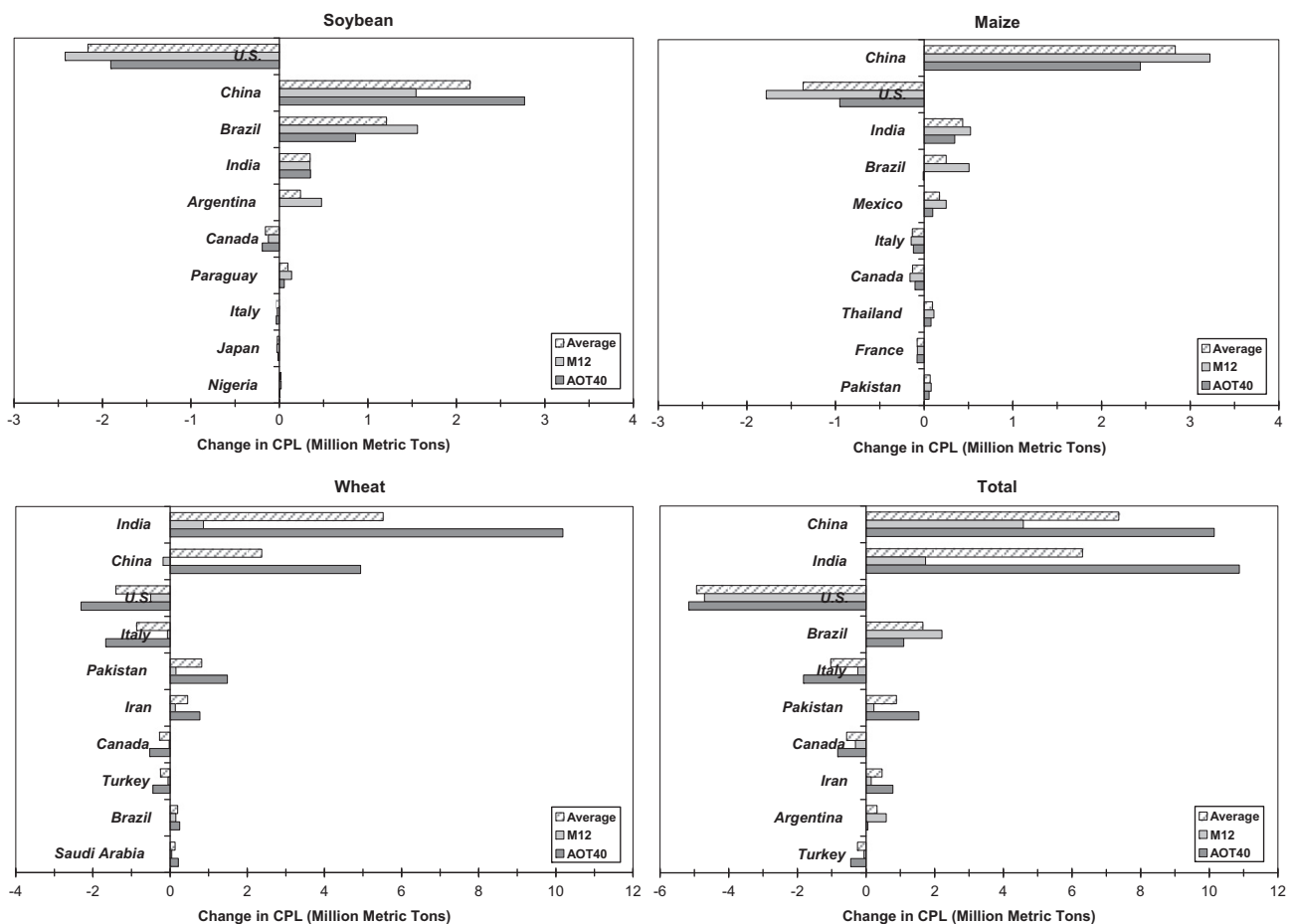


Fig. 9. Change in crop production loss (CPL, million metric tons) for the ten countries with highest absolute difference in estimated mean CPL between 2000 and 2030 under the B1 scenario using the M12 and AOT40 metrics for a) soybean, b) maize, c) wheat, and d) total CPL.

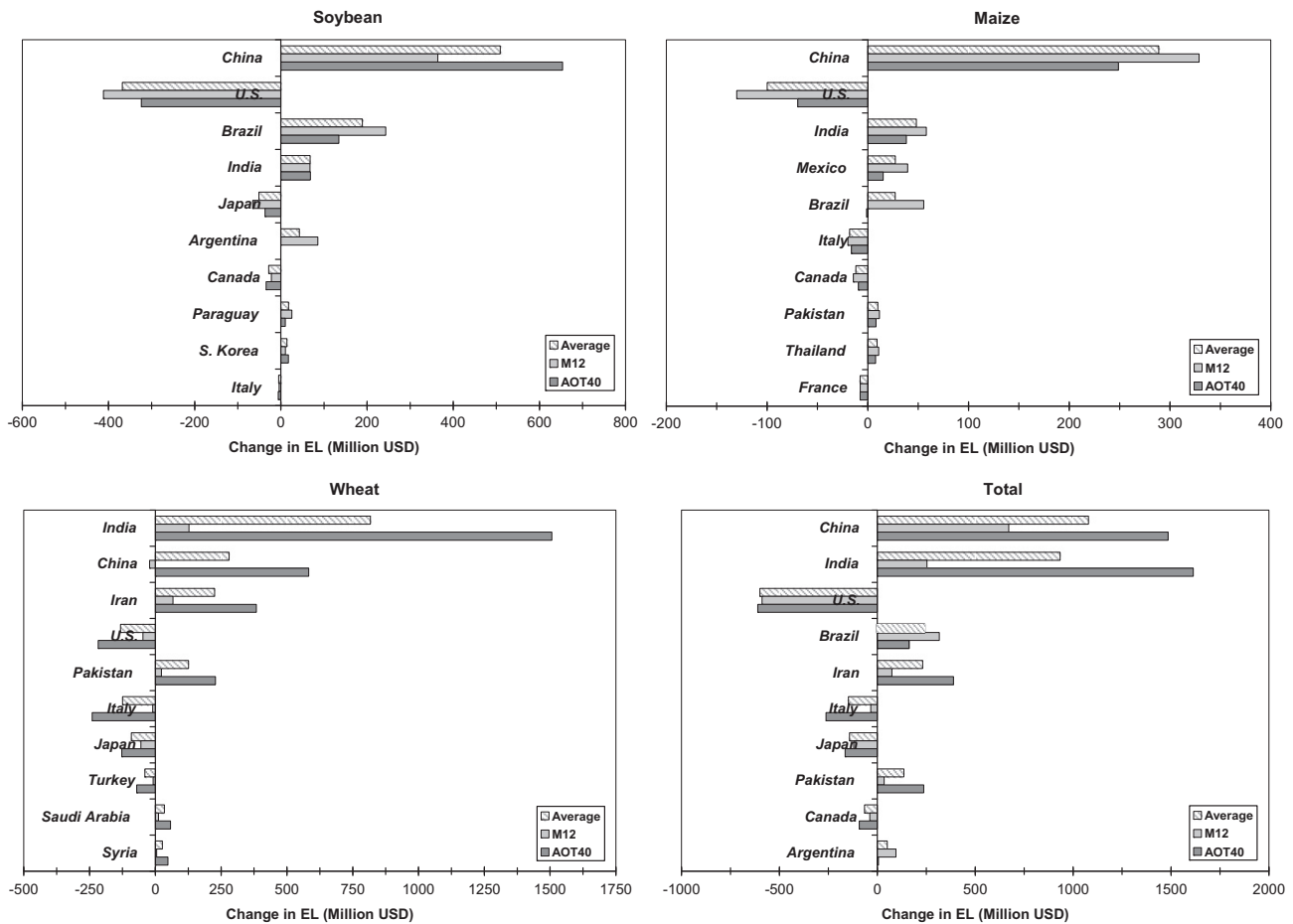


Fig. 10. Change in economic loss (EL, million USD₂₀₀₀) for the ten countries with highest absolute difference in estimated mean EL between 2000 and 2030 under the B1 scenario using the M12 and AOT40 metrics for a) soybean, b) maize, c) wheat, and d) total EL.

bioengineering, the historical rate of crop yield improvements experienced since the Green Revolution is declining in many parts of the world, and that the genetic ceiling for maximal yield potential is being approached despite increasing inputs (Peng et al., 1999; Duvick and Cassman, 1999; Tilman et al., 2002). Ozone mitigation provides a means to increase this “ceiling” and the efficiency by which crops use nitrogen, water, and land. Moreover, with mounting evidence that crop yield improvements from CO₂ fertilization may not be as great as previously expected (Long et al., 2005) and that O₃ pollution may more than offset even significant crop yield gains due to climate change in some regions (Reilly et al., 2007), surface O₃ abatement provides a critical opportunity to increase supplies of food and fuel without further environmental degradation. Because tropospheric ozone is a potent greenhouse gas in addition to a noxious air pollutant (Forster et al., 2007), O₃ reductions would also provide numerous co-benefits to climate and human health (West et al., 2006, 2007; Fiore et al., 2008; Anenberg et al. 2010). Ozone abatement measures could further benefit climate in the absence of an explicit climate change mitigation policy, since many O₃ precursors are emitted by the same sources as CO₂ and other long-lived greenhouse gases.

5. Conclusions

In this study we estimated the global risk to three key staple crops (soybean, maize, and wheat) of surface ozone pollution in the near future (year 2030) using simulated O₃ concentrations

under two scenarios of projected O₃ precursor emissions (the IPCC SRES A2 and B1 storylines), two metrics of O₃ exposure (M12 and AOT40), field-based CR relationships, and global maps of agricultural production compiled from satellite data and census yield statistics. We find that for the A2 scenario, global year 2030 relative yield loss of wheat ranges from 5.4 to 26% (a further reduction in yield of +1.5–10% from year 2000 values), 15–19% for soybean (+0.9–11%), and 4.4–8.7% for maize (+2.1–3.2%), with total crop production losses worth \$17–35 USD₂₀₀₀ annually (+\$6–17 billion in losses). In the B1 scenario, we estimate that global relative yield loss totals 4.0–17% for wheat (a decrease in yield of +0.1–1.8% from year 2000 values), 9.5–15% for soybean (+0.7–1.0%), and 2.5–6.0% for maize (+0.3–0.5%), with total losses worth \$12–21 billion annually (+\$1–3 billion). Our crop production and economic loss estimates should be considered conservative given their derivation from observation-based, year 2000 crop production data that likely underestimate actual agricultural production in the year 2030.

Acknowledgements

We thank N. Ramankutty and C. Monfreda for providing us with pre-publication access to their global crop area and yield datasets. We also thank two anonymous reviewers for their thoughtful comments and suggestions, which greatly improved the quality of this paper. S. Avnery was supported by the NASA Earth and Space Science Fellowship Program, Grant NNX10A971H.

Appendix. Supplementary material

Supplementary data associated with this article can be found, in the on-line version, at doi:10.1016/j.atmosenv.2011.01.002.

References

- Adams, R.M., Glycer, J.D., Johnson, S.L., McCarl, B.A., 1989. A reassessment of the economic effects of ozone on United States agriculture. *Journal of the Air Pollution Control Association* 39, 960–968.
- Anenberg, S.C., Horowitz, L.W., Tong, D.Q., West, J.J., 2010. An estimate of the global burden of anthropogenic ozone and fine particulate matter on premature human mortality using atmospheric modeling. *Environmental Health Perspectives* 118, 1189–1195.
- Avnery, S., Mauzerall, D.L., Liu, J., Horowitz, L.W., 2011. Global crop yield reductions due to surface ozone exposure: 1. Year 2000 crop production losses and economic damage. *Atmospheric Environment* 45, 2284–2296.
- Beig, G., et al., 2008. Threshold exceedances and cumulative ozone exposure indices at tropical suburban site. *Geophysical Research Letters* 35, L02802. doi:10.1029/2007GL031434.
- Booker, F.L., et al., 2009. The ozone component of global change: potential effects on agricultural and horticultural plant yield, product quality and interactions with invasive species. *Journal of Integrative Plant Biology* 51, 337–351.
- Brasseur, G.P., et al., 2006. Impact of climate change on the future chemical composition of the global troposphere. *Journal of Climate* 19, 3932–3951.
- Dentener, F., et al., 2005. The impact of air pollutant and methane emission controls on tropospheric ozone and radiative forcing: CTM calculations for the period 1990–2030. *Atmospheric Chemistry and Physics* 5, 1731–1755.
- Dentener, F., et al., 2006. The global atmospheric environment for the next generation. *Environmental Science and Technology* 40, 3586–3594.
- Duvick, D.N., Cassman, K.G., 1999. Post-green-revolution trends in yield potential of temperature maize in the north-central United States. *Crop Science* 39, 1622–1630.
- Edgerton, M.D., 2009. Increasing crop productivity to meet global needs for feed, food, and fuel. *Plant Physiology* 149, 7–13.
- FAO. FAOSTAT, Food and Agricultural Organization of the United Nations. Available at: <http://faostat.fao.org/> (accessed May, 2008).
- Feng, Z., Kobayashi, K., 2009. Assessing the impacts of current and future concentrations of surface ozone on crop yield with meta-analysis. *Atmospheric Environment* 43, 1510–1519.
- Fiore, A., et al., 2008. Characterizing the tropospheric ozone response to methane emission controls and the benefits to climate and air quality. *Journal of Geophysical Research* 113, D08307. doi:10.1029/2007JD009162.
- Fiore, A., et al., 2009. Multimodel estimates of intercontinental source–receptor relationships for ozone pollution. *Journal of Geophysical Research* 114, D04301. doi:10.1029/2008JD010816.
- Fiscus, E.L., Booker, F.L., Burkey, K.O., 2005. Crop responses to ozone: uptake, modes of action, carbon assimilation and partitioning. *Plant, Cell and Environment* 28, 997–1011.
- Fishman, J., et al., 2010. An investigation of widespread ozone damage to the soybean crop in the upper Midwest determined from ground-based and satellite measurements. *Atmospheric Environment* 44, 2248–2256.
- Forster, P., et al., 2007. Changes in atmospheric constituents and radiative forcing. In: Solomon, S., et al. (Eds.), *Climate Change 2007: The Physical Science Basis*. Contribution of Working Group I to the Fourth Assessment Report of the Intergovernmental Panel on Climate Change. Cambridge University Press, Cambridge, United Kingdom and New York, NY, USA.
- Fuhrer, J., 2009. Ozone risk for crops and pastures in present and future climates. *Naturwissenschaften* 96, 173–194.
- Heagle, A.S., 1989. Ozone and crop yield. *Annual Review of Phytopathology* 27, 397–423.
- Heck, W.W., 1989. Assessment of crop losses from air pollutants in the United States. In: MacKenzie, J.J., El-Ashry, M.T. (Eds.), *Air Pollution's Toll on Forests and Crops*. Yale University Press, New Haven, pp. 235–315.
- Horowitz, L.W., et al., 2003. A global simulation of tropospheric ozone and related tracers: description and evaluation of MOZART, Version 2. *Journal of Geophysical Research* 108 (D24), 4784. doi:10.1029/2002JD002853.
- Horowitz, L.W., 2006. Past, present, and future concentrations of tropospheric ozone and aerosols: methodology, ozone evaluation, and sensitivity to aerosol wet removal. *Journal of Geophysical Research* 111, D22211. doi:10.1029/2005JD006937.
- Hough, A.D., Derwent, R.G., 1990. Changes in the global concentration of tropospheric ozone due to human activities. *Nature* 344, 645–650.
- Jacob, D., Winner, D., 2009. Effect of climate change on air quality. *Atmospheric Environment* 43, 51–63.
- Karenlampi, L., Skarby, L., 1996. Critical Levels for Ozone in Europe: Testing and Finalizing the Concepts. Department of Ecology and Environmental Science, University of Kuopio, 363 pp.
- Kiehl, J.T., et al., 1998. The national center for atmospheric research community climate model: CCM3. *Journal of Climate* 11, 1131–1149.
- Krupa, S.V., Nosal, M., Legge, A.H., 1998. A numerical analysis of the combined open-top chamber data from the USA and Europe on ambient ozone and negative crop responses. *Environmental Pollution* 101, 157–160.
- Lesser, V.M., Rawlings, J.O., Spruill, S.E., Somerville, M.C., 1990. Ozone effects on agricultural crops: statistical methodologies and estimated dose–response relationships. *Crop Science* 30, 148–155.
- Levy II, H., et al., 2008. Strong sensitivity of late 21st century climate to projected changes in short-lived air pollutants. *Journal of Geophysical Research* 113, D06102. doi:10.1029/2007JD009176.
- Long, S.P., Ainsworth, E.A., Leakey, A.D., Morgan, P.B., 2005. Global food insecurity: treatment of major food crops with elevated carbon dioxide or ozone under large-scale fully open-air conditions suggests recent models may have over-estimated future yields. *Philosophical Transactions of the Royal Society B* 360, 2011–2020.
- Marengo, A., Gouget, H., Nédélec, P., Pagés, J.-P., Karcher, F., 1994. Evidence of a long-term increase in tropospheric ozone from Pic du Midi data series: consequences: positive radiative forcing. *Journal of Geophysical Research* 99, 16617–16632.
- Mauzerall, D.L., Wang, X., 2001. Protecting agricultural crops from the effects of tropospheric ozone exposure: reconciling science and standard setting in the United States, Europe and Asia. *Annual Review of Energy and the Environment* 26, 237–268.
- Mills, G., et al., 2007. A synthesis of AOT40-based response functions and critical levels of ozone for agricultural and horticultural crops. *Atmospheric Environment* 41, 2630–2643.
- Ming, Y., Ramaswamy, V., 2009. Nonlinear climate and hydrological responses to aerosol effects. *Journal of Climate* 22. doi:10.1175/2008JCLI2362.1.
- Monfreda, C., Ramankutty, N., Foley, J.A., 2008. Farming the planet: 2. Geographic distribution of crop areas, yields, physiological types, and net primary production in the year 2000. *Global Biogeochemical Cycles* 22, GB1022. doi:10.1029/2007GB002947.
- Morgan, P.B., Mies, T.A., Bollero, G.A., Nelson, R.L., Long, S.P., 2006. Season-long elevation of ozone concentration to projected 2050 levels under fully open-air conditions substantially decreases the growth and production of soybean. *New Phytologist* 170, 333–343.
- Nakićenović, N., et al., 2000. Emissions Scenarios: a Special Report of Working Group III of the Intergovernmental Panel on Climate Change. Cambridge Univ. Press, New York, 599 pp.
- Oltmans, S.J., et al., 2006. Long-term changes in tropospheric ozone. *Atmospheric Environment* 40, 3156–3173.
- Peng, S., et al., 1999. Yield potential of trends of tropical rice since the release of IR8 and the challenge of increasing rice yield potential. *Crop Science* 39, 1552–1559.
- Ramankutty, N., Evan, A., Monfreda, C., Foley, J.A., 2008. Farming the planet: 1. Geographic distribution of global agricultural lands in the year 2000. *Global Biogeochemical Cycles* 22, GB1003. doi:10.1029/2007GB002952.
- Riahi, K., Grübler, A., Nakićenović, N., 2007. Scenarios of long-term socio-economic and environmental development under climate stabilization. *Technological Forecasting and Social Change* 74, 887–935.
- Reidmiller, D.R., et al., 2009. The influence of foreign vs. North American emissions on surface ozone in the U.S. *Atmospheric Chemistry and Physics* 9, 5027–5042.
- Reilly, J., et al., 2007. Global economic effects of changes in crops, pasture, and forests due to changing climate, carbon dioxide, and ozone. *Energy Policy* 35, 5370–5383.
- Tilman, D., et al., 2001. Forecasting agriculturally driven global environmental change. *Science* 292, 281–284.
- Tilman, D., et al., 2002. Agricultural sustainability and intensive production practices. *Nature* 418, 671–677.
- USDA, United States Department of Agriculture, 1994. Major world crop areas and climatic profiles. In: *Agricultural Handbook No. 664*. World Agricultural Outlook Board, U.S. Department of Agriculture Available at: <http://www.usda.gov/oce/weather/pubs/Other/MWCACP/MajorWorldCropAreas.pdf>.
- USDA FAS, United States Department of Agriculture Foreign Agricultural Service. Country Information. Available at: <http://www.fas.usda.gov/countryinfo.asp> (accessed May 2008).
- United States Census Bureau, June 2010. International Database. <http://www.census.gov/ipc/www/idb/worldpopgraph.php>.
- Van Dingenen, R., Raes, F., Krol, M.C., Emberson, L., Cofala, J., 2009. The global impact of O₃ on agricultural crop yields under current and future air quality legislation. *Atmospheric Environment* 43, 604–618.
- Wang, X., Mauzerall, D.L., 2004. Characterizing distributions of surface ozone and its impact on grain production in China, Japan and South Korea: 1990 and 2020. *Atmospheric Environment* 38, 4383–4402.
- West, J.J., Fiore, A.M., Naik, V., Horowitz, L.W., Schwarzkopf, M.D., Mauzerall, D.L., 2007. Ozone air quality and radiative forcing consequences of changes in ozone precursor emissions. *Geophysical Research Letters* 34, L06806. doi:10.1029/2006GL029173.
- West, J.J., Fiore, A.F., Horowitz, L.W., Mauzerall, D.L., March 14, 2006. Mitigating ozone pollution with methane emission controls: global health benefits. *Proceedings of the National Academy of Science* 103 (11).
- Westenbarger, D.A., Frisvold, G.B., 1995. Air pollution and farm-level crop yields: an empirical analysis of corn and soybeans. *Agricultural and Resource Economics Review* 24, 156–165.
- Wu, S., et al., 2008. Effects of 2000–2050 global change on ozone air quality in the United States. *Journal of Geophysical Research* 113, D06302.